

Surfactant Ligand Removal and Rational Fabrication of Inorganically Connected Quantum Dots

Haitao Zhang,[†] Bo Hu,[†] Liangfeng Sun,^{†,||} Robert Hovden,[‡] Frank W. Wise,[‡] David A. Muller,^{‡,§} and Richard D. Robinson^{*,†}

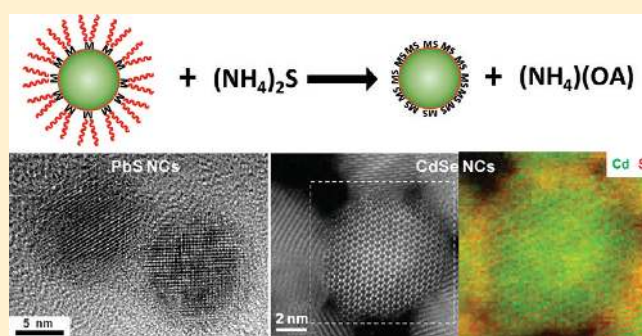
[†]Department of Materials Science and Engineering and [‡]School of Applied and Engineering Physics, Cornell University, Ithaca, New York 14853, United States

[§]Kavli Institute at Cornell for Nanoscale Science, Ithaca, New York 14853, United States

S Supporting Information

ABSTRACT: A novel method is reported to create inorganically connected nanocrystal (NC) assemblies for both II–VI and IV–VI semiconductors by removing surfactant ligands using $(\text{NH}_4)_2\text{S}$. This surface modification process differs from ligand exchange methods in that no new surfactant ligands are introduced and the post-treated NC surfaces are nearly bare. The detailed mechanism study shows that the high reactivity between $(\text{NH}_4)_2\text{S}$ and metal–surfactant ligand complexes enables the complete removal of surfactant ligands in seconds and converts the NC metal-rich shells into metal sulfides. The post-treated NCs are connected through metal–sulfide bonding and form a larger NCs film assembly, while still maintaining quantum confinement. Such “connected but confined” NC assemblies are promising new materials for electronic and optoelectronic devices.

KEYWORDS: Nanocrystals, ligand removal, mechanism, connection, quantum confinement, photoluminescence lifetime



Inorganic colloidal nanocrystals (NCs) have attracted much attention in the past decade due to their unique size and shape-dependent properties.¹ Thin films of semiconductor NCs have emerged as promising new materials for electronic and optoelectronic devices.^{2–11} In most successful synthetic routes to colloidal NCs, the use of bulky hydrocarbon (C_8 – C_{18}) molecules with coordinating functional groups (such as $-\text{COOH}$, $-\text{NH}_2$, etc.) as surfactant ligands is crucial for stabilization, for prevention of aggregation, and for size and shape control of NCs.^{12–15} The presence of these large organic molecules, however, creates highly insulating barriers which block electronic communication between NCs, limiting the usefulness of colloidal NCs assemblies in applications. Thermal removal of surfactant ligands has proven to be difficult because NCs become unstable at temperatures well below those required for the pyrolysis of surfactant ligands.¹⁶ Research into surface modification of NCs has thus mainly focused on replacing the long chain ligands with small molecules, such as amines,^{3,16} thiols,¹⁷ and hydrazine.⁴ More recently, the ligand exchange reactions have been extended to use inorganic surfactant ligands, including $\text{BF}_4 \cdot \text{NO}$,¹⁸ metal chalcogenides,^{19–21} and metal-free chalcogenides.²² These surfactant ligand modifications have decreased the interparticle distances and, in several cases, introduced conductive inorganic ligands, resulting in NCs thin films with increased conductance.

To this point, chemical NC surface modifications have followed a “ligand exchange” strategy, that is, using a new ligand A to replace

the original ligand B. But some NCs, such as lead chalcogenide (IV–VI) semiconductors, are difficult to be stabilized by small surfactant ligands^{18,22} and tend to lose original sizes and shapes upon ligand exchange. In this work, we report a novel method to completely remove bulky surfactant ligands from both II–VI and IV–VI semiconducting NCs films using a simple metal-free chalcogenide compound, $(\text{NH}_4)_2\text{S}$. This surface modification process differs significantly from other reported “ligand exchange” methods in that no new surfactant ligands are introduced and the post-treated NC surfaces are nearly bare. The detailed mechanism study shows that the high reactivity between $(\text{NH}_4)_2\text{S}$ and metal–surfactant ligand complexes enables the complete removal of the bulky surfactant ligands in seconds and converts the NCs metal-rich surface shells into metal sulfides (Figure 1), resulting in a more stoichiometric NC product where metal cations and chalcogenide anions are nearly balanced. This surface modification process produces unique NCs assemblies in which the NCs are inorganically connected through metal–sulfide bonding but still retain quantum confinement. Photoluminescence lifetime studies show that the inorganic connection between NCs causes increased electronic coupling, which leads to exciton dissociation.

Received: August 20, 2011

Revised: October 10, 2011

Published: October 19, 2011

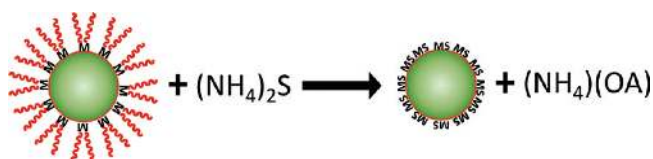


Figure 1. Schematic of NCs surfactant ligand removal using $(\text{NH}_4)_2\text{S}$. For clarity, the surface metal-rich layer is simplified as $\text{M}(\text{OA})_2$ ($\text{M} = \text{Pb}, \text{Cd}$).

Table 1. Summary of $(\text{NH}_4)_2\text{S}$ Treatment Conditions for PbS NC Films

conditions	PbS NC film thickness (nm)	$(\text{NH}_4)_2\text{S}$ concentration (M)	$(\text{NH}_4)_2\text{S}$ treat time (s)
1	120	0.004	10
2	120	0.004	30
3	120	0.004	120
4	120	0.100	30
5	40	0.004	5
6	20	0.004	2

The ligand removal is performed by dipping a NC film into a dilute $(\text{NH}_4)_2\text{S}$ methanol solution. In a typical experiment, a spin-coated ca. 120 nm thick PbS NC (with oleate surfactant ligands) film on a substrate (Si or glass slide) is dipped into a 0.004 M $(\text{NH}_4)_2\text{S}$ methanol solution for 30 s (condition 2, Table 1), followed by washing in methanol for 30 s, to remove any $(\text{NH}_4)_2\text{S}$ and the replaced organic ligand residues. After ligand removal, the NCs film is no longer soluble in any nonpolar or polar solvents. The treated nanoparticles retain their original sizes and shapes (Figure 2a–d), while the NC films exhibit some cracking due to the reduction of interparticle spacing (Figure 2a). According to small-angle X-ray scattering (SAXS) studies (Figure 2e), the center-to-center distance of PbS nanoparticles (6 ± 0.5 nm) decreases from 7.3 ± 0.1 to 5.8 ± 0.1 nm. Transmission electron microscopy (TEM) studies on the monolayer film clearly show that the NCs are connected by direct attachment after $(\text{NH}_4)_2\text{S}$ treatment (Figure 2c,d).

Micro CHN elemental analysis reveals a sharp decrease in carbon content (Table S1, Supporting Information), from 11.26% (wt %, as-synthesized NCs) to 0.51% (after ligand removal) for 6 nm PbS NCs, which confirms that most of surfactant ligands are removed. The amount of surfactant ligands present can be assessed using Fourier transform infrared spectroscopy (FTIR), by comparing the intensity of C–H stretching while normalizing by the NCs core exciton absorption. Figure 2f shows the FTIR spectra of PbS NCs (11.1 ± 1.2 nm) before and after ligand removal under several reaction conditions (Table 1). A significant decrease on intensity of bands between 3300 and 3700 nm, which corresponds to C–H stretching, and a red shift of the excitonic peak from 2023 to 2087 nm are observed after treatment of a 120 nm thick NCs film in 0.004 M $(\text{NH}_4)_2\text{S}$ for 10 s (condition 1). TEM images show no noticeable size change in the NCs before and after the $(\text{NH}_4)_2\text{S}$ treatment. The excitonic peak red shift can be explained by the partial leakage of the wave functions into neighboring NCs due to the removal of insulating surfactant ligands, which relaxes the quantum confinement.¹⁹ Increasing $(\text{NH}_4)_2\text{S}$ treatment time to 30 s (condition 2) results in a bigger excitonic peak red shift (2140 nm) and weaker C–H

stretching, indicating more surfactant ligands are removed. However, condition 2 represents the maximum of surfactant ligand removal: the excitonic peak is not further red-shifted and the C–H stretching intensity does not further decrease (Figure S1, Supporting Information) for longer treatment times (condition 3) or for higher concentrations of $(\text{NH}_4)_2\text{S}$ solution at the 30 s treatment time (condition 4).

The organic residues on PbS NCs (11.1 nm) after $(\text{NH}_4)_2\text{S}$ treatment exhibit different C–H stretching characteristics to those of oleate ligands. Figure 2g shows the normalized C–H stretching peaks before and after ligand removal under different conditions. A shoulder peak at ca. 3330 nm is characteristic of the –CH=CH– group of the oleate ligand and is clearly visible in the spectrum of as-synthesized PbS NCs (I). We also note that the $(\text{NH}_4)_2\text{S}$ solution cannot destroy the –CH=CH– group of oleate ligands under our reaction conditions (Figure S2, Supporting Information). Thus, the disappearance of the 3330 nm shoulder peak after $(\text{NH}_4)_2\text{S}$ treatment 2 in III proves that the oleate surfactant ligands have been completely removed and the remaining C–H stretching originates from a different organic species.

The same conclusion can also be drawn from thermogravimetric (TGA) analyses (Figure 2h). The total weight loss of the post-treated PbS NCs (3.5%) is much lower than that of the original sample (24.3%, Figure S3 in the Supporting Information), further suggesting that most of the surfactant ligands have been removed. The organic residues, however, display a different thermal decomposition model from that of the oleate surfactant ligands: after $(\text{NH}_4)_2\text{S}$ treatment, the organic residues are removed completely below 190 °C, but in the as-synthesized PbS NCs most of oleate ligands do not begin decomposition until 250 °C. These data again show that the organic residues on post-treated NCs surface are not oleate ligands but are more volatile species. Although we cannot exclude the possibility that the surfactant ligand removal may generate hydrocarbon fragments binding to NCs, these new organic species could also be solvent methanol molecules. Methanol is a strong coordinating ligand toward Lewis acidic metal centers and thus can form coordinating bonds to coordinatively unsaturated surface Pb atoms after surfactant ligand removal. The same solvent absorption on NCs surfaces has been observed in previous surfactant ligand exchange reactions.¹⁶ Such solvent coordination may help to stabilize the post-treated NCs and prevent decomposition into bulk materials.

The efficacy of the ligand removal is highly related to the thickness of the NCs films. On the basis of FTIR studies, under identical concentrations of $(\text{NH}_4)_2\text{S}$ solution (0.004 M), it takes 30 s to completely remove the oleate ligands from a ca. 120 nm film, while only 5 s is needed for ca. 40 nm films (Figure S4a,b in the Supporting Information, condition 5 of Table 1). When the thickness of the film is decreased to ca. 20 nm, the oleate ligands can be completely removed in only 2 s (Figure S4c,d in the Supporting Information, condition 6 of Table 1). These results suggest that the reactions between $(\text{NH}_4)_2\text{S}$ and surfactant ligands are highly favorable, and the whole ligand removal process is controlled by the $(\text{NH}_4)_2\text{S}$ solution diffusion.

This surfactant ligand removal technique can be expanded to other semiconducting NCs, such as PbSe, CdS, CdSe, and CdSe/CdS core/shell nanoparticles. Different chalcogenide salts show a similar reactivity toward $(\text{NH}_4)_2\text{S}$. FTIR studies reveal the significant decrease on C–H stretching peak and the disappearance of the oleate ligands after $(\text{NH}_4)_2\text{S}$ treatment (Figure S5, Supporting Information). Noticeable decreases in the total

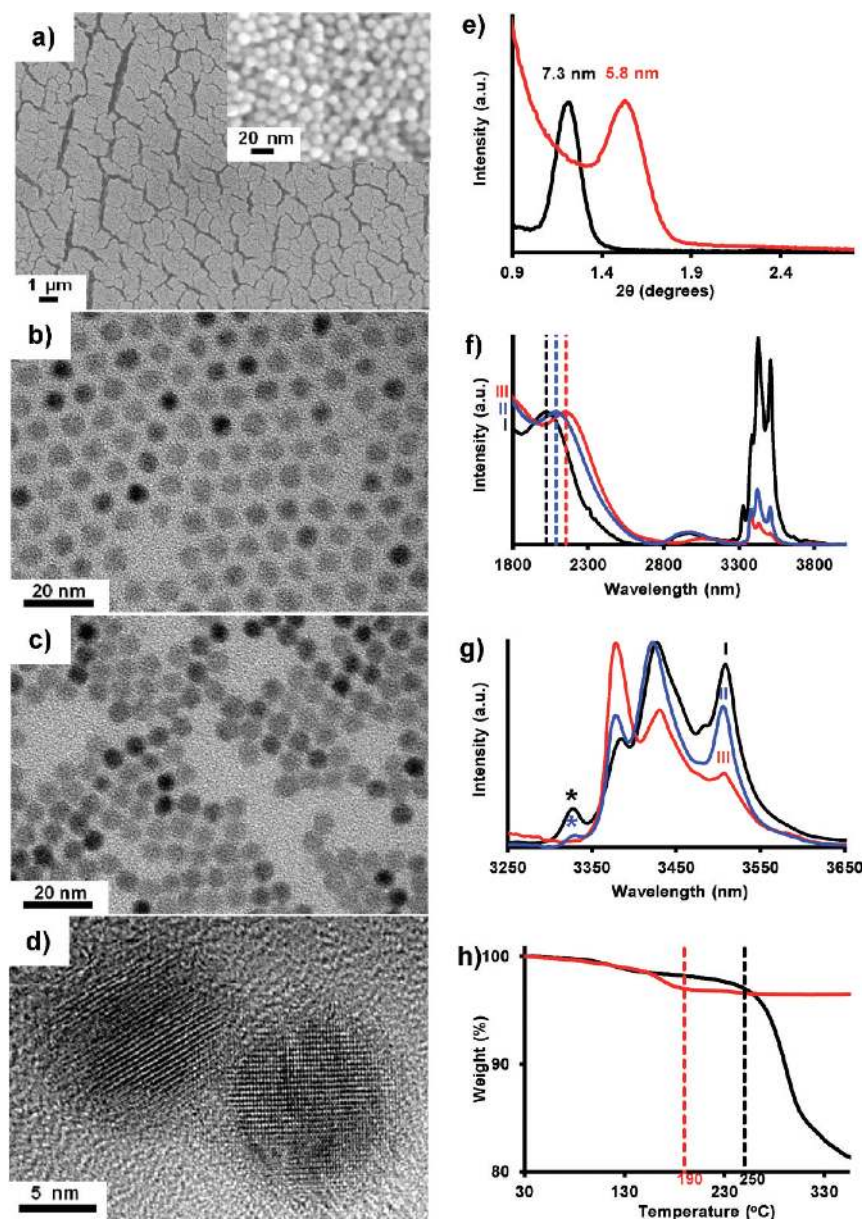


Figure 2. a) SEM image of 120 nm thick PbS NC (11.1 nm) film after $(\text{NH}_4)_2\text{S}$ treatment (condition 2). Inset of (a) shows that PbS NCs still retain original sizes and shapes after ligand removal. (b, c) TEM images of monolayer films of PbS NCs (6 nm) before (b) and after (c) surfactant ligand removal. (d) HRTEM image of PbS NCs (11.1 nm) after surfactant ligand removal shows that the PbS NCs are connected. (e) SAXS data of PbS NCs (6 nm) before (black) and after (red) ligand removal. (f) FTIR spectra of 120 nm thick film of PbS NCs (11.1 nm) before (I) and after (II, III) ligand removal under different conditions: spectrum II is condition 1; III is condition 2. The spectra are each normalized by the intensity of their NCs absorption peak. (g) The normalized C–H stretching peaks of I–III. The shoulder peak at ca. 3330 nm is marked by * in I and II, corresponding to the $(-\text{CH}=\text{CH}-)$ group of oleate ligand. (h) TGA scans of PbS (6 nm) NCs before (black) and after ligand removal (red).

weight loss in TGA studies are also observed (Figure S6, Supporting Information). Similar to the PbS NCs, all the post-treated semiconducting NCs films lost solubility in both polar and nonpolar solvents. TEM studies show that nanoparticles are connected after $(\text{NH}_4)_2\text{S}$ treatment, while retaining original sizes and shapes (Figure S7, Supporting Information).

A striking property of these connected NCs is that they still maintain quantum confinement. All the studied semiconducting NCs preserve the size-dependent optical absorption features after ligand removal (Figure 3, also see Figure 1f and Figure S4 and Figure S5a in the Supporting Information) and a red shift is observed—due to the relaxing of quantum confinement, caused

by the removal of insulating surfactant ligands. Figure S8 (Supporting Information) shows the XRD patterns of a variety of NCs before and after $(\text{NH}_4)_2\text{S}$ treatment. Scherrer analyses on the distinguishable peaks do not reveal noticeable crystal size changes.

Although inorganic chalcogenide compounds have been successfully used as surfactant ligands to stabilize colloidal NCs, the ligand exchange mechanism, as well as the chemical compositions of inorganic surfactant ligands that bind to NCs, remain unclear. We attempt to clarify the mechanism of our surfactant ligands removal reactions using a number of techniques. Elemental analyses of $(\text{NH}_4)_2\text{S}$ treated PbS NCs (6 nm) reveal an increase of S content (Table S1, Supporting Information),

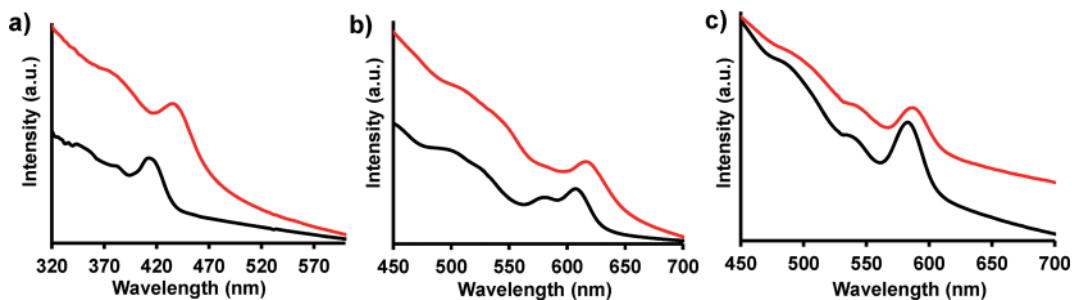


Figure 3. Optical absorption spectra of thin films of CdS (3.5 nm, a), CdSe (4.7 nm, b), and CdSe-CdS core-shell NCs (4.4 nm, c) before (black) and after (red) ligand removal. Upon surfactant ligands removal, excitonic peaks show red shifts of 19, 10, and 4 nm for CdS, CdSe, and CdSe-CdS core-shell NCs, respectively.

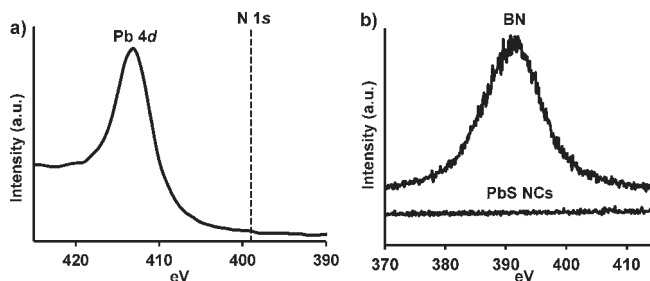
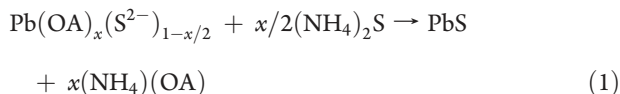


Figure 4. No nitrogen signal is detected in XPS (a) and WDS (b) analyses on PbS (6 nm) NCs after ligand removal. The dashed line in (a) shows the position of missing N 1s peak. In (b) the top spectrum shows the nitrogen peak of standard sample boron nitride (BN), and the bottom line is the spectrum of PbS NCs after ligand removal, which does not show any nitrogen signal.

resulting in Pb:S ratios that are changed from 1:0.826 (as-synthesized NCs) to 1:1.098 (after $(\text{NH}_4)_2\text{S}$ treatment), while no detectable amount of N is observed. The absence of N atoms is further confirmed by X-ray photoelectron spectroscopy (XPS) (Figure 4a) and wavelength dispersive X-ray spectroscopy (WDS) analyses (Figure 4b). The lack of a characteristic peak at ca. 3920 nm in FTIR spectra of the $(\text{NH}_4)_2\text{S}$ treated NCs also excludes the presence of a $-\text{S}-\text{H}$ group. All these data indicate that our surfactant ligand removal process strips the organics and adds a small amount of S^{2-} atoms onto the NCs (Figure 1) and that no inorganic ligands— $(\text{NH}_4)_2\text{S}$ or $(\text{NH}_4)\text{S}^-$ —exist on the surface of the NCs. It is well accepted that PbS NCs passivated with oleate ligands contain a Pb-rich surface layer,²³ in which the Pb atoms coordinate to both OA^- ligands and S^{2-} anions. We can describe the stoichiometry of these Pb species as $\text{Pb}^{2+}(\text{OA}^-)_x(\text{S}^{2-})_{1-x/2}$ ($0 < x < 2$). Thus, the whole ligand removal process can be described as



or for clarity, we can rewrite eq 1 as



This process represents a novel chemical surface modification of colloidal nanocrystals that does not rely on the conventional ligand exchange reactions which use a new (smaller) ligand to replace the original surfactant ligands. In our ligand removal, we perform an efficient chemical reaction on the surface layer of

NCs that not only removes the surfactant ligands but also changes the NCs chemical composition (Figure 1).

The structure and chemical compositions of CdSe NCs after $(\text{NH}_4)_2\text{S}$ treatment are determined with atomic resolution using high-angle annular dark-field (HAADF) imaging and electron energy loss spectroscopic (EELS) mapping in an aberration-corrected electron microscope.²⁴ HAADF images reveal that CdSe NCs are connected to each other with a solid inorganic bridge after $(\text{NH}_4)_2\text{S}$ treatment (Figure 5a and Figure S9a in the Supporting Information). Such connection is similar to the previously reported oriented attachment of PbSe²⁵ and CdTe²⁶ NCs, but in our case we do not observe any preferred orientation and thus there are two discrete connected NCs lattices instead of a newly formed single crystal. The chemical compositions are mapped from the EELS signal over multiple nanoparticles, clearly displaying the presence of an S-rich surface layer (Figure 5b and Figure S9b in the Supporting Information), and a heavy presence of S in the bridging regions. Cadmium is also present in this S-rich surface. Mapping of the Cd and Se atoms shows Cd-rich and Se-poor connections between NCs (Figure 5c). From this it appears that the newly formed cadmium sulfide surface layer is important for the connection of CdSe NCs. These results explicitly confirm our reaction mechanism, that is, $(\text{NH}_4)_2\text{S}$ removes the surfactant ligands by a chemical reaction that converts the metal-surfactant ligand complexes into metal-sulfides.

We also demonstrate that the metal-oleate complexes are very reactive toward $(\text{NH}_4)_2\text{S}$: when $(\text{NH}_4)_2\text{S}$ is added to a $\text{Pb}(\text{OA})_2$ toluene solution, a quantitative amount of PbS forms nearly spontaneously, with the purity of PbS product confirmed by XRD analysis (Figure S10a, Supporting Information). A similar reaction between $(\text{NH}_4)_2\text{S}$ and $\text{Cd}(\text{OA})_2$ also results in a quantitative yield of CdS (Figure S10b, Supporting Information). Such a high reactivity between $(\text{NH}_4)_2\text{S}$ and metal-oleate complexes should be the major driving force for this efficient ligand removal.

The $(\text{NH}_4)_2\text{S}$ treatment results in NCs which lack the protection of “real” surfactant ligands. On such a nearly bare NC surface, the coordinatively unsaturated M-S ($M = \text{metal}$) species tend to form new M-S bonding to the neighboring NCs to fulfill coordination numbers. The NCs are thus connected by the interparticle M-S bonding. We have found that $(\text{NH}_4)_2\text{S}$ treated NCs films do not redisperse into any polar or nonpolar solvents and, upon sonication, exist as small pieces of broken films (Figure S11, Supporting Information), suggesting that the NCs are no longer discrete units but part of a larger NCs assembly. Such connections can be clearly observed in the

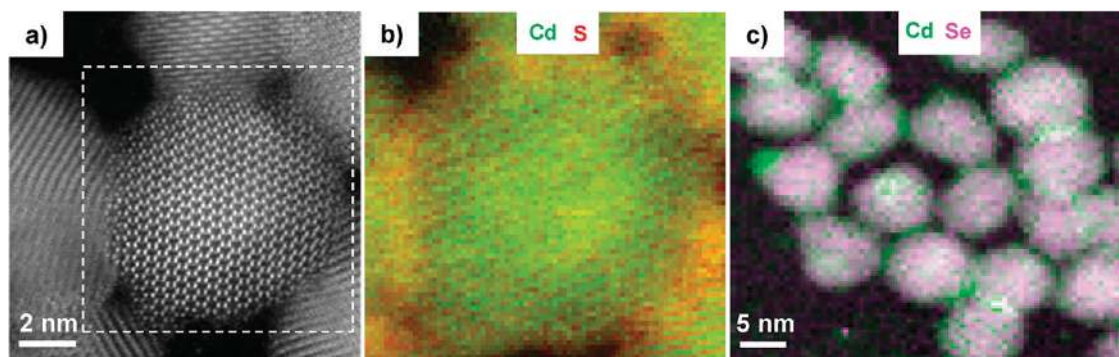
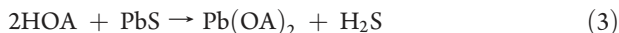
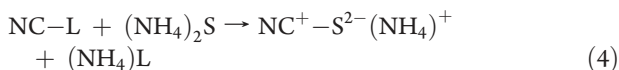


Figure 5. STEM HAADF image of CdSe NCs (8.1 nm) after $(\text{NH}_4)_2\text{S}$ treatment showing the NCs are connected to each other with inorganic bridging (a). EELS mapping using the sulfur $L_{2,3}$, cadmium $M_{4,5}$, and selenium $L_{2,3}$ edges inside the dashed white line square area of (a) reveals the presence of a sulfur-rich surface layer (b). Cadmium is also present in the sulfur-rich surface area, where the concentration of Se is very low (c).

TEM and HAADF images (Figure 2c,d, Figure 5, and Figures S7 and S9 in the Supporting Information). The formation of the larger NCs assembly may provide further stabilization on the NCs and prevent the decomposition into bulk materials. The NCs maintain the assembly matrix even after addition of organic surfactant ligands such as oleyamine, TOPO, and TOP. The addition of oleic acid, however, does redissolve the PbS NCs film into soluble separate NCs, but the NCs are smaller in size than the original NCs (Figures S12, Supporting Information). Oleic acid can etch PbS (eq 3), thus it is able to break the metal–sulfide bonding between NCs.



In a newly published report,²² Talapin et al. demonstrated that cadmium chalcogenides NCs can be stabilized by $(\text{NH}_4)_2\text{S}$ in highly polar solvents such as formamide via ligand exchange reactions. They proposed that S^{2-} ions bind to NCs surface and provide electrostatic stabilization for colloidal dispersion, while the negative charges are balanced by cation NH_4^+ . We can describe this process as (L = surfactant ligand)



Compared to eq 2, a major difference in eq 4 is that one $(\text{NH}_4)_2\text{S}$ only replaces one L^- surfactant ligand, representing an incomplete reaction between $(\text{NH}_4)_2\text{S}$ and NC-L complexes. Considering $(\text{NH}_4)_2\text{S}$ is used in excess in both Talapin's work and our synthesis, the different reactivity of $(\text{NH}_4)_2\text{S}$ in eq 4 and eq 2 can be explained by the solvent effect: the highly polar solvent (formamide, $\epsilon = 106$) used in Talapin's work can provide strong solvation to the $(\text{NH}_4)^+$ cation and stabilize it, favoring the formation of $-\text{S}^{2-} \cdot (\text{NH}_4)^+$ pairs on the NCs surface. In our reactions, however, methanol ($\epsilon = 33$) is a much weaker polar solvent and cannot provide enough stabilization for $(\text{NH}_4)^+$ cations, resulting in a complete reaction of $(\text{NH}_4)_2\text{S}$ with organic surfactant ligands that leads to the formation of metal sulfides, as we have described in eq 2 and Figure 1. It is worth noting that Talapin et al. also found that polarity of solvents played an important role in their $(\text{NH}_4)_2\text{S}$ ligand exchange reactions and lower NC colloidal stability was observed in solvents of lower polarity.²²

The surfactant ligand removal and the interconnection of NCs significantly influence the photoluminescence (PL). Figure 6a shows the PL spectra of PbS NCs (5.5 ± 0.4 nm) before and after

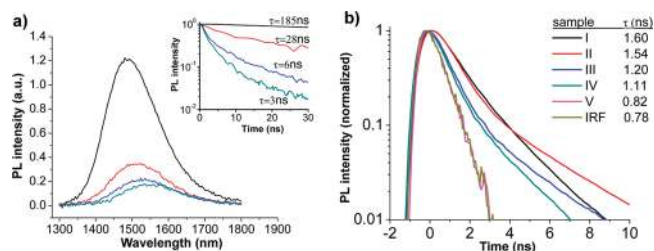


Figure 6. (a) PL spectra and lifetime of ca. 120 nm thick films of PbS NCs (5.5 nm) before (black) and after 0.004 M $(\text{NH}_4)_2\text{S}$ treatment for 2 (red), 10 (blue), and 30 s (aqua). Inset: measured PL transients, with lifetime of fastest component in the decay indicated. (b) PL lifetimes of ca. 120 nm thick films of CdSe/CdS NCs (4.4 nm): I, with the original surfactant ligands; II, after treatment in 0.1 M mercaptoethanol for 1 min; III, after treatment in 0.004 M $(\text{NH}_4)_2\text{S}$ for 30 s and then in 0.1 M mercaptoethanol for 1 min; IV, after treatment in 0.004 M $(\text{NH}_4)_2\text{S}$ for 30 s and then in 0.1 M mercaptoethanol for 5 min; V, after treatment in 0.004 M $(\text{NH}_4)_2\text{S}$ for 30 s. The instrument response function (IRF) is also shown in the figure.

$(\text{NH}_4)_2\text{S}$ treatment under different conditions, with the corresponding fluorescence transients (inset). The PL was measured with fixed excitation level (<1 electron–hole pair per NC), and PL lifetimes were recorded at the peak of the PL spectrum. Similar to the absorption spectra, the PL peaks exhibit a clear red shift upon ligand removal. The integrated PL intensity decreases as the surfactant ligands are removed. The fluorescence transients (Figure 6) do not exhibit single-exponential decays, which suggests that multiple processes are involved in the decays. The PL lifetime is about 185 ns for the original NC films. After complete removal of the surfactant ligands, the fastest component in the PL decay has a lifetime of 3 ns. There are two processes that should be considered for the dramatic variation of the PL lifetime. First, we expect that surface defects generated by the ligand removal will quench the PL and decrease the lifetime. The second process is the increased electronic coupling between NCs, which leads to dissociation of photocreated excitons in films of coupled NCs. To clarify the origin of the fast fluorescence decay, we repeated the experiments (Figure 6b) using CdSe/CdS core/shell NCs (4.4 ± 0.4 nm) because surface defects in this system can be repaired by treatment with mercaptoethanol.²⁷ The PL lifetime of the CdSe/CdS core/shell NCs decreases significantly upon $(\text{NH}_4)_2\text{S}$ treatment (Figure 6b, samples I and V), which is similar to the trend observed with the PbS NCs.

The PL lifetime of the original CdSe/CdS NCs treated with mercaptoethanol is almost the same as that before the treatment (samples I and II), indicating that mercaptoethanol molecules can passivate the NCs surface well. FTIR spectra confirm that the original surfactant ligands are completely replaced by mercaptoethanol. Applying this surface repair process to the $(\text{NH}_4)_2\text{S}$ treated CdSe/CdS NCs shows an increase in the PL lifetime (sample III) and C–H stretching peak intensity (Figure S13, Supporting Information). The C–H stretching increase confirms the binding of mercaptoethanol to the $(\text{NH}_4)_2\text{S}$ -treated CdSe/CdS NCs. The lifetime of sample III, however, is still less than that of sample II. We note that the 1 min and 5 min treatments with mercaptoethanol produce virtually the same lifetime (samples III and IV), which indicates that the surface defects on $(\text{NH}_4)_2\text{S}$ -treated CdSe/CdS NCs have been repaired as best they can be under our conditions. Compared to sample II, the PL lifetime shortening of sample III is likely caused by electronic coupling of the NCs since the surface defects have already been suppressed by the mercaptoethanol ligands. Thus, we conclude that the rapid fluorescence quenching observed in the CdSe/CdS samples after ligand removal can be attributed at least partially to exciton dissociation. Further work will be needed to determine the relative rates of electron trapping and tunneling to adjacent NCs in PbS NCs. A similar dramatic decrease of the PL lifetime of PbS NCs was observed when oleic acid ligands were replaced by shorter linker molecules, and exciton dissociation was confirmed by the direct observation of free electrons in the film.²⁸ Thus, there is reason to expect strong electronic coupling in the $(\text{NH}_4)_2\text{S}$ treated PbS NC films, but this must be verified.

In conclusion, we have demonstrated a novel method to create assemblies of inorganically connected NCs that retain quantum confinement. The high reactivity between $(\text{NH}_4)_2\text{S}$ and metal–surfactant ligand complexes enables the complete removal of the bulky surfactant ligands from semiconductor NCs films in seconds and converts the NCs metal-rich surface shells into metal sulfides. Unlike the other ligand exchange methods, this surface modification removes the original surfactant ligands without introducing new ligands, and the surfaces of post-treated NCs are nearly bare. The bare NCs are connected through metal–sulfide bonding and form a larger NCs assembly, while still maintaining quantum confinement. Such “connected but confined” NCs assemblies are promising new materials for electronic and optoelectronic devices.

■ ASSOCIATED CONTENT

S Supporting Information. Materials, nanocrystal synthesis, characterization techniques described in the text, elemental analysis results, additional FTIR and XRD spectra, additional TGA diagrams, and additional TEM and STEM HAADF images. This material is available free of charge via the Internet at <http://pubs.acs.org>.

■ AUTHOR INFORMATION

Corresponding Author

*E-mail: rdr82@cornell.edu.

Present Addresses

^{||}Department of Physics and Astronomy, Bowling Green State University, Bowling Green, Ohio, 43402, United States.

■ ACKNOWLEDGMENT

We acknowledge helpful discussions with Professor Tobias Hanrath. This publication is based on work supported in part by Award No. KUS-C1-018-02, made by King Abdullah University of Science and Technology (KAUST) and by the Semiconductor Research Corporation and the Center for Nanoscale Systems (NSF #EEC-0117770, 0646547). We also acknowledge support of Cornell Center for Materials Research (CCMR) with funding from the Materials Research Science and Engineering Center program of the National Science Foundation (cooperative agreement DMR 0520404), and support of Energy Materials Center at Cornell (EMC²), an Energy Frontier Research Center funded by the U.S. Department of Energy, Office of Science, Office of Basic Energy Science under Award Number DE-SC0001086.

■ REFERENCES

- (1) Alivisatos, A. P. *Science* **1996**, *271*, 933–937.
- (2) Ridley, B. A.; Nivi, B.; Jacobson, J. M. *Science* **1999**, *286*, 746–749.
- (3) Yu, D.; Wang, C. J.; Guyot-Sionnest, P. *Science* **2003**, *300*, 1277–1280.
- (4) Talapin, D. V.; Murray, C. B. *Science* **2005**, *310*, 86–89.
- (5) Urban, J. J.; Talapin, D. V.; Shevchenko, E. V.; Kagan, C. R.; Murray, C. B. *Nat. Mater.* **2007**, *6*, 115–121.
- (6) Colvin, V. L.; Schlamp, M. C.; Alivisatos, A. P. *Nature* **1994**, *370*, 354–357.
- (7) Coe, S.; Woo, W. K.; Bawendi, M.; Bulovic, V. *Nature* **2002**, *420*, 800–803.
- (8) Jarosz, M. V.; Porter, V. J.; Fisher, B. R.; Kastner, M. A.; Bawendi, M. G. *Phys. Rev. B* **2004**, *70*, 195327.
- (9) Gur, I.; Fromer, N. A.; Geier, M. L.; Alivisatos, A. P. *Science* **2005**, *310*, 462–465.
- (10) Huynh, W. U.; Dittmer, J. J.; Alivisatos, A. P. *Science* **2002**, *295*, 2425–2427.
- (11) Nozik, A. J.; Beard, M. C.; Luther, J. M.; Law, M.; Ellingson, R. J.; Johnson, J. C. *Chem. Rev.* **2010**, *110*, 6873–6890.
- (12) Yin, Y.; Alivisatos, A. P. *Nature* **2005**, *437*, 664–670.
- (13) Peng, X. G.; Manna, L.; Yang, W. D.; Wickham, J.; Scher, E.; Kadavanich, A.; Alivisatos, A. P. *Nature* **2000**, *404*, 59–61.
- (14) Punties, V. F.; Krishnan, K. M.; Alivisatos, A. P. *Science* **2001**, *291*, 2115–2117.
- (15) Baranov, D.; Manna, L.; Kanaras, A. G. *J. Mater. Chem.* **2011**, *21*, 16694–16703.
- (16) Law, M.; Luther, J. M.; Song, O.; Hughes, B. K.; Perkins, C. L.; Nozik, A. J. *J. Am. Chem. Soc.* **2008**, *130*, 5974–5985.
- (17) Luther, J. M.; Law, M.; Song, Q.; Perkins, C. L.; Beard, M. C.; Nozik, A. J. *ACS Nano* **2008**, *2*, 271–280.
- (18) Dong, A. G.; Ye, X. C.; Chen, J.; Kang, Y. J.; Gordon, T.; Kikkawa, J. M.; Murray, C. B. *J. Am. Chem. Soc.* **2011**, *133*, 998–1006.
- (19) Kovalenko, M. V.; Scheele, M.; Talapin, D. V. *Science* **2009**, *324*, 1417–1420.
- (20) Kovalenko, M. V.; Bodnarchuk, M. I.; Zausseil, J.; Lee, J. S.; Talapin, D. V. *J. Am. Chem. Soc.* **2010**, *132*, 10085–10092.
- (21) Lee, J.-S.; Kovalenko, M. V.; Huang, J.; Chung, D. S.; Talapin, D. V. *Nanotechnol.* **2011**, *6*, 348–352.
- (22) Nag, A.; Kovalenko, M. V.; Lee, J.-S.; Liu, W.; Spokoyny, B.; Talapin, D. V. *J. Am. Chem. Soc.* **2011**, *133*, 10612–10620.
- (23) Fu, H.; Tsang, S.-W.; Zhang, Y.; Ouyang, J.; Lu, J.; Yu, K.; Tao, Y. *Chem. Mater.* **2011**, *23*, 1805–1810.
- (24) Muller, D. A.; Kourkoutis, L. F.; Murfitt, M.; Song, J. H.; Hwang, H. Y.; Silcox, J.; Dellby, N.; Krivanek, O. L. *Science* **2008**, *319*, 1073–1076.
- (25) Cho, K. S.; Talapin, D. V.; Gaschler, W.; Murray, C. B. *J. Am. Chem. Soc.* **2005**, *127*, 7140–7147.
- (26) Tang, Z. Y.; Kotov, N. A.; Giersig, M. *Science* **2002**, *297*, 237–240.
- (27) Hohng, S.; Ha, T. *J. Am. Chem. Soc.* **2004**, *126*, 1324–1325.
- (28) Choi, J. J.; Luria, J.; Hyun, B.-R.; Bartnik, A. C.; Sun, L.; Lim, Y.-F.; Marohn, J. A.; Wise, F. W.; Hanrath, T. *Nano Lett.* **2010**, *10*, 1805–1811.